# Dynamic tensile behaviour at low temperature of CFRP using a split Hopkinson pressure bar

T. Gómez-del Río [a], E. Barbero [b], R. Zaera [b], C. Navarro [b,*]

[a] *Materials Science and Engineering Group, High School of Experimental Sciences and Technology, Rey Juan Carlos University, Tulipán s/n 28933 Móstoles Madrid, Spain*

[b] *Department of Continuum Mechanics and Structural Analysis, University Carlos III of Madrid, Avda. de la Universidad 30, 28911 Leganés, Madrid, Spain*

**Abstract**

This paper deals with the effect of temperature (room and low temperatures) on the tensile properties at high strain rates of CFRP laminates. Dynamic tests were performed on different carbon/epoxy laminates configurations: unidirectional, $[0]_{10}$ and $[90]_{10}$, and quasi isotropic $[\pm 45/0/90]_S$. All these tests were carried out at two temperatures: 20 and 60 °C. Validation of Hopkinson bar theory using one dimensional wave propagation theory was performed by analysing the effect of low temperature on elastic wave propagation along the bars of the experimental device, and the subsequent wave dispersion phenomena. The value of the strain on the specimen derived from the signals recorded at the bar gauges was compared with that obtained from a gauge glued on the specimen. All the experimental results of the response of CFRPs at high strain rates and low temperature are analysed and discussed.

*Keywords:* A. Polymer matrix composites; B. Stress/strain curves; B. Mechanical properties; Split Hopkinson bar

## 1. Introduction

Fibre reinforced composite materials (FRPs) are widely used in high technology structural applications, on account of their high stiffness, high strength and low density, especially in applications, such as aeronautic and aerospace, in which the ratio stiffness/weight and strength/weight are critical [1]. In some of these applications, structures may be subjected to impulsive loading such as the impact of debris during take off or landing of a plane, or to the release of a turbine blade. The mechanical response (load-deformation relationship and failure) of composite materials may be sensitive to the loading rate. A full characterization of the behaviour of FRPs under dynamic has prompted numerous investigations in recent years [2 5]. But further, more research is still required [2].

Because of the experimental difficulties involved, few reliable data are available. Much of the work on the dynamic properties of composite materials was in bending at medium strain rate using Charpy pendulum and Drop Weight Tower devices [6,7]. Although relatively high strain rates can be achieved with these techniques, difficulties arise from the existence of non-uniform stress fields and multiple types of damage [8], which hinder the fundamental formulation of strain rate effects on material properties [9]. So test specimens should be subjected to homogeneous state of stress, such as the uniaxial tensile test, to determine the effect of strain rate on the mechanical behaviour of composite materials. One

* Corresponding author. Tel.: +34 91 624 94 91; fax: +34 91 624 94 30.

*E mail address:* navarro@ing.uc3m.es (C. Navarro).

way to get a uniaxial homogeneous state of stress at high rates is by using the split Hopkinson pressure bar, which is the most widely used experimental technique to investigate material behaviour at high strain rates. This device was first introduced by Kolsky [10] in the split compression version. Other compression [11,12], shear and torsion [13 15], tensile [16], flexural and fracture [17 19] and even biaxial [20] versions have been developed over the last decades.

Several authors report dynamic tensile test on CFRPs using a split Hopkinson pressure bar at room temperature [2,4,21 24]. On unidirectional laminates, most of the results showed no effect of strain rate on the Young modulus and tensile strength in the fibre direction, while others detected a slight strain rate effect on theses properties, either a decrease [17] or an increase [8]. On quasi-isotropic and woven laminates, a significant rise of stiffness and strength were observed [21,24].

In aeronautical and aerospace applications, structural components made of CFRPs laminates may be subjected to low temperatures. Low temperatures may modify the mechanical properties [25] for two reasons: first, the changes of the mechanical properties of the matrix and the fibres with temperature, and second, the thermal stresses due to the mismatch of the thermal expansion coefficient of each constituent. The latter will affect the tensile strength of the composite laminate [26]. Most studies have focused on static properties, such as the influence of low temperature on the Young modulus [27] and shear modulus [28] at temperatures over −150 °C. However, little has been published on CFRP behaviour at high strain rates and at low temperatures, as stated in some recent papers [29], probably due to the great difficulty in obtaining valid results.

With the Hopkinson bar, the need to cooling down the specimen requires the coupling of a non-standard climatic chamber to the set-up. If an adhesive clamping system is used to connect the specimen to the bar, the low temperature gives rise to an embrittlement of the joining materials. A direct strain measurement on the specimen involves the use of special strain gages and adhesives. Dispersive wave effects could become important at low temperature, given the variation of elastic properties and geometry of the bars.

This study examines the mechanical behaviour of carbon fibre reinforced epoxy laminates at high strain rate and low temperature, by means of uniaxial tensile tests using a split Hopkinson pressure bar with different stacking sequences: unidirectional (in fibre and transverse direction) and quasi-isotropic. Different specimen bar clamping systems were tried to select the most appropriate for this materials and thermal conditions. The effect of temperature on elastic wave propagation on the bars was evaluated, together with the applicability of the classical Hopkinson bar theory to obtain actual stress strain curves. Finally, the influence of low temperature (down to −60 °C) on the dynamic properties of CFRPs was studied.

## 2. Experimental methods

### 2.1. Experimental set-up

Dynamic tensile tests were performed using a modified tensile split Hopkinson bar as sketched in Fig. 1. The device consists of a gas gun, an input bar and an output bar, the supports, and a data acquisition system. Both bars are of high-yield silver-steel, 22 mm in diameter and 1 m long, and they can move horizontally without any restriction.

The experimental set-up works in the following way: an air gun that impels a projectile against one end of the incident bar connector and generates a tensile pulse which travels along the incident bar. When this pulse reaches the specimen, partial is reflected, and partial is transmitted to the specimen and to the output bar. The stress pulses in the bars are measured by strain gages (VISHAY CEA-06-12UN-350) attached to the bars at the central point. The strain gage signals are recorded using a VISHAY 2200 signal conditioner and a TEKTRONIX TDS 420A digital oscilloscope with 1 ls time increment for data point acquisition.

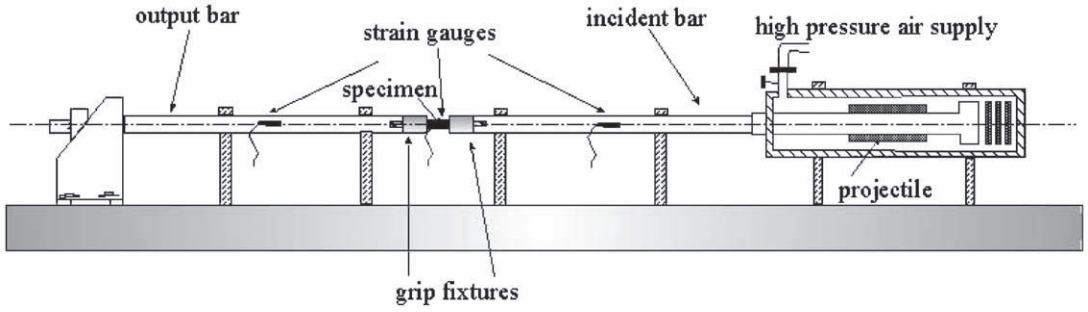


Fig. 1. Sketch of the tensile split Hopkinson bar device.

The projectile is launched at a few metre per second. In all the tests of this work the projectile was impelled at 10 m/s.

To reach low temperatures in the specimen a climatic chamber was specially designed to be coupled to the Hopkinson bar device, in such a way that a portion of the input and output bars remained inside it. The chamber has two circular holes through which the bars pass during the test. The whole set-up is shown in Fig. 2. Liquid nitrogen flows inside the chamber, controlled by an electrovalve connected to a low temperature thermocouple placed close to the specimen. A fan inside the chamber ensures a uniform distribution of temperature, and the specimen was cooled during 20 min before testing to reach the thermal equilibrium with the environment. This exposure time was obtained from a thermal numerical analysis of the heat transmission process in the specimen.

### 2.2. Specimen bars fixture

For testing metallic materials, cylindrical dog-bone-shaped specimens are usually screwed to the bars. This type of specimen bar union ensures a good transmission of the waves; however, clamping CFRP specimens to the bars is not an easy because of their plane geometry and high Young modulus and tensile strength; this fact is even more difficult at low temperatures. Thus an alternate clamping method had to be designed that would alter the wave shape as little as possible before it reaches the specimen.

Mechanical grips were tried, like those used in static tests, to join the specimen to the bar [30], but we observed a systematic slip of the specimen or matrix fibre shear failure. Other mechanical clamping devices were developed, two of them are shown in Fig. 3, but these introduced noise in the pulses recorded by the bars strain gages, probably due to looseness of the specimen inside the clamps which weakens transmission of the waves.

Fig. 2. Experimental set up.

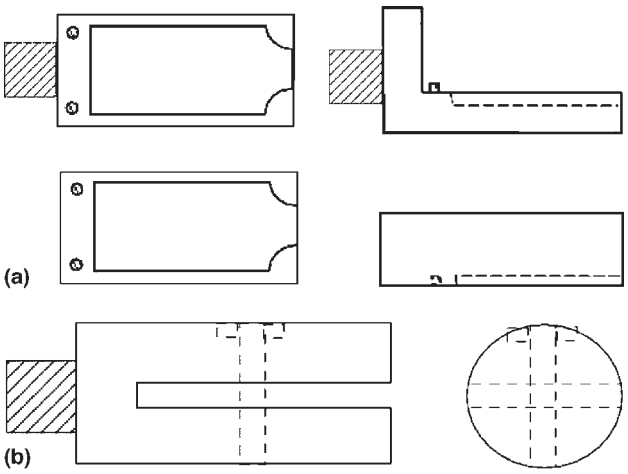


Fig. 3. Mechanical clamping devices developed for testing CFRP laminates: (a) union by machining a bas relief of the specimen end; (b) union by bolt.

Finally, we adopted a gluing technique. A epoxy adhesive was used with 20 MPa shear strength at 20 °C. The fixtures to hold the specimen were 22 mm diameter silver-steel cylinders, of the same material and diameter as the input and output bars to reduce reflections. One end had a thread to be screwed to the bars and the other a slot 40 mm long and 3 mm thick (Fig. 4). This slot length ensures the appropriate strength at the adhesive laminate interface.

Alignment of the specimen is a key point of the tensile test of a laminate, especially for unidirectional ones. This was achieved by using the device shown in Fig. 5. Both the fixture cylinders and the specimen are placed inside the alignment device during the curing process of the adhesive.

### 2.3. Specimen geometry and materials

All laminates were manufactured by SACESA (Spain), following all the requirements of the aeronautic industry, using AS4/3501-6 Hexcel prepegs with a volumetric fibre content of 60%. Two configurations were tested in this work: unidirectional, both in fibre ($[0]_{10}$) and transverse direction ($[90]_{10}$), and quasi-isotropic $[\pm 45/0/90]_S$. The static mechanical properties of the tape ply at room temperature are summarized in Table 1.

When designing the shape and size of the specimen, it should be short enough to reach stress equilibrium as soon as possible and its cross-section must be reduced to ensure its failure before any debonding of the adhesive layer. Additionally, due to the laminate heterogeneity, it should be large enough to have mechanical properties representative of the material. From the static

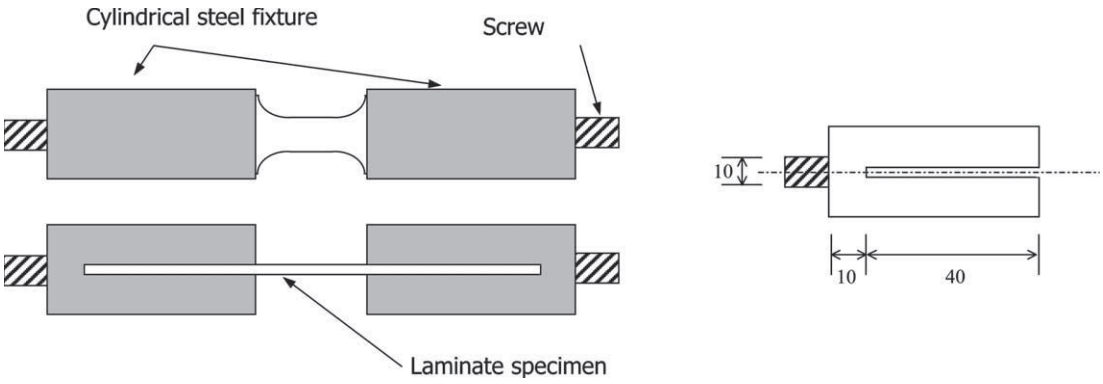


Fig. 4. Assembly of the fixture and specimen (lengths in mm).

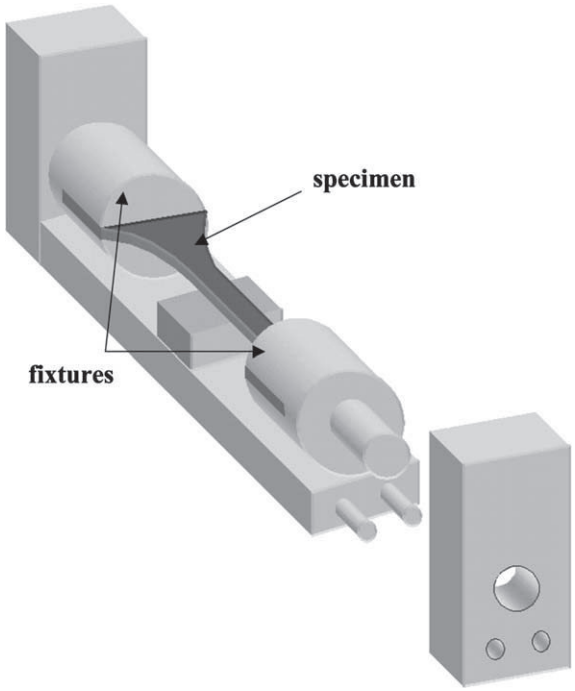


Fig. 5. Alignment device for CFRP laminate dynamic testing using a tensile Hopkinson bar.

Table 1
Mechanical properties of AS4/3501 6 ply at room temperature

| Property | Tape AS4/3501 6 |
|---|---|
| 0° Tensile modulus (GPa) | 131 |
| 90° Tensile modulus (GPa) | 9 |
| 0° Tensile strength (MPa) | 2137 |
| 90° Tensile strength (MPa) | 80 |

*Source*: Ref. [37].

mechanical properties of the laminates, the shape and the dimensions of the specimens were estimated (Fig. 6).

Specimen thicknesses are shown in Table 2. The thickness of the unidirectional laminate $[0]_{10}$ is decreased to 1 mm in the gage length to avoid shear failure at the specimen widening.

## 3. Data analysis

From the one-dimensional wave propagation theory, the dynamic stress strain response of the specimen may be derived from strain histories in a section of the bars [31]. The strain gage in the middle of the incident bar (Fig. 7) measures the sum of the incident wave $e_i$ plus the reflected wave $e_r$. The gage in the middle of the output bar measures in the transmitted wave $e_t$. The strain gage in incident bar was placed at a distance from the specimen to avoid interferences of the first pulses.

Using subscripts 1 and 2 to refer to the two specimen ends (Fig. 7), the displacements $u$ of such sections are given by

$$u_1 = \int_0^t c_0\varepsilon_1(\tau)\,\mathrm{d}\tau, \quad u_2 = \int_0^t c_0\varepsilon_2(\tau)\,\mathrm{d}\tau, \tag{1}$$

where $c_0$ is the sound speed in the bars material and $t$ is the time elapsed from the beginning of the test. Eq. (1) could be written in terms of the incident, reflected and transmitted pulses at the specimen ends

$$u_1 = c_0\int_0^t (\varepsilon_{1i}(\tau) - \varepsilon_{1r}(\tau))\,\mathrm{d}\tau,$$
$$u_2 = c_0\int_0^t \varepsilon_{2t}(\tau)\,\mathrm{d}\tau, \tag{2}$$

where stresses and strains are assumed positive in tension. The average strain in the specimen is

$$\varepsilon_p(t) = \frac{u_1(t) - u_2(t)}{L} = -\frac{c_0}{L}\int_0^t (\varepsilon_{1i}(\tau) - \varepsilon_{1r}(\tau) - \varepsilon_{2t}(\tau))\,\mathrm{d}\tau, \tag{3}$$

where $L$ is the specimen length. The forces at the ends of the specimen are obtained from

$$F_1 = EA(\varepsilon_{1i} + \varepsilon_{1r}), \quad F_2 = EA\varepsilon_{2t}, \tag{4}$$

where $E$ and $A$ are, respectively, Young's modulus and the cross-sectional area of the Hopkinson bars. Assuming equilibrium in the specimen, that is $F_1 = F_2$, then

$$\varepsilon_{1i}(t) + \varepsilon_{1r}(t) = \varepsilon_{2t}(t). \tag{5}$$

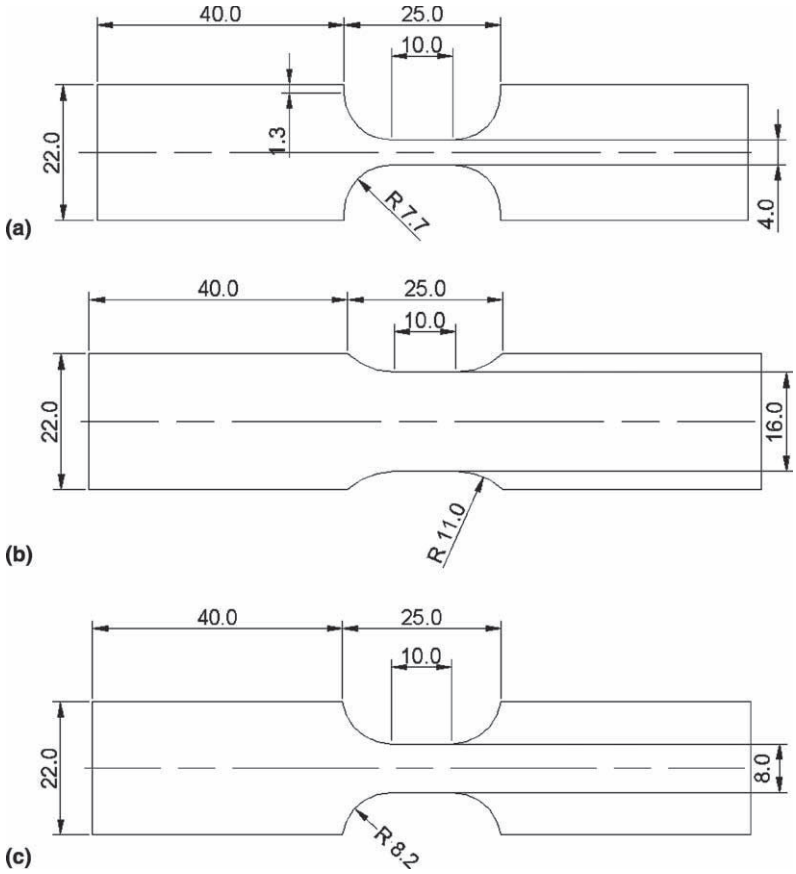


Fig. 6. Dimensions of specimens (mm): (a) unidirectional laminate $[0]_{10}$; (b) unidirectional laminate $[90]_{10}$; (c) quasi isotropic laminate $[\pm 45/0/90]_S$.

Table 2
Specimen thicknesses

| Laminate | Thickness (mm) |
|---|---|
| Unidirectional $[0]_{10}$ | 2.0 (1.0 in the gage length) |
| Unidirectional $[90]_{10}$ | 2.0 |
| Quasi isotropic $[\pm 45/0/90]_S$ | 1.6 |

Finally stress, strain and strain rate in the specimen could be derived as

$$\sigma_p(t) = E \cdot \frac{A}{A_p} \cdot \varepsilon_{2t}(t) \tag{6}$$

$$\varepsilon_p(t) = \frac{2 \cdot c_o}{L} \cdot \int_0^t \varepsilon_{1r}(\tau)\, d\tau \tag{7}$$

$$\dot{\varepsilon}_p(t) = \frac{2 \cdot c_o}{L} \cdot \varepsilon_{1r}(t) \tag{8}$$

where $A_p$ is the specimen cross-sectional area.

This conventional technique involves the one-dimensional wave propagation theory in bars behaving elastically. According to this theory, a wave propagating in the bar is not affected by the wave dispersion. Indeed, it is considered that the phase velocity of such a wave does not depend on the wave frequency. Moreover, material damping or inelastic effects are neglected and,

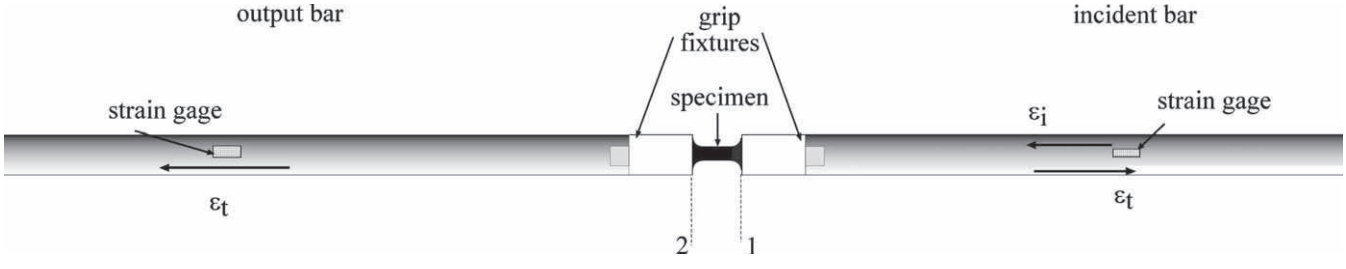


Fig. 7. Measure of the strain in the Hopkinson bar device.

therefore, no wave attenuation occurs. Thus, for a single wave propagating in one direction, the knowledge of the longitudinal strain pulse at a given cross-section gives the strain at another cross-section by time shifting, with no change of its shape.

However, the specific characteristic of the tensile testing of thin laminates at low temperature can distort the pulses, and a verification of the hypothesis conventionally adopted is required. Possible distortion of the pulses could be caused by:

- fixture device, specially the adhesive layer;
- square cross-section of the specimen;
- bar impedance variation due to cooling.

Also, wave dispersion caused by the spread of phase velocities over the signal was examined.

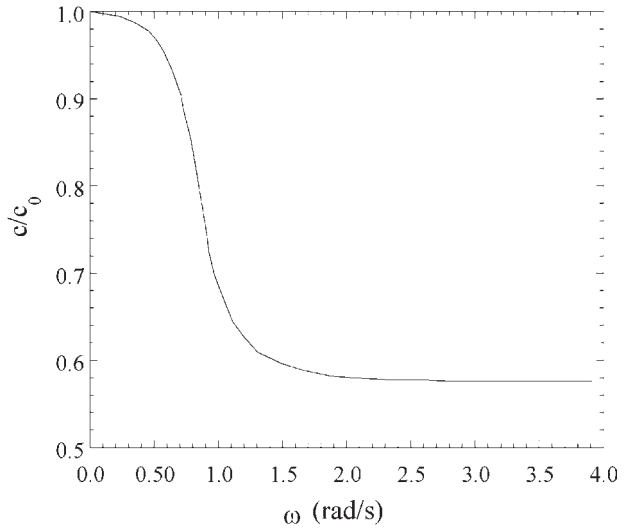


Fig. 8. Wave propagation velocity versus angular frequency according to Bancroft [34].

### 3.1. Wave dispersion effects

The one-dimensional elastic wave theory is valid only if wave dispersion due to three-dimensional effects (radial inertia of the bars) can be neglected. However, the phase velocity depends on the frequency and the waves would not propagate without dispersion. The dispersive nature of wave propagation in rods was first described by Pochhammer [32], and Love [33] developed the theory related to this phenomena. Using the numerical solution proposed by Bancroft [34], the velocity of longitudinal wave $c$ and the velocity of a wave of infinite wavelength $c_0$ could be related by the following equation:

$$\frac{c}{c_0} = D\left(\frac{R}{\lambda}, v\right), \tag{9}$$

where $k$ is the corresponding wave-length, $m$ is the Poisson ratio and $R$ is the bar radius. The result of Bancroft's equation in terms of angular frequency $x$ is shown in Fig. 8.

The wave dispersion produces a difference between the shape of the pulse measured at the strain gage location and that in the bar end. To evaluate this effect in the stress strain curve, the shape of the pulses at the bar ends was determined using Bancroft's equation. Taking the origin at the middle point of the bars, where the strain gage was placed, the incident bar end is located at $x = L_b/2$ and the output bar end at $x = -L_b/2$, $L_b$ being the bar length.

The strain at a section $x$ of the incident bar can be expressed in the frequency domain as

$$\tilde{\varepsilon}(x,\omega) = \tilde{P}_i(\omega)\cdot e^{-\gamma(\omega)\cdot x} + \tilde{P}_r(\omega)\cdot e^{\gamma(\omega)\cdot x}, \tag{10}$$

where $\tilde{P}_i(\omega)$ and $\tilde{P}_r(\omega)$ are, respectively, the Fourier transforms of the measured incident and the reflected strain pulses, and $c(x)$ is the propagation coefficient given by

$$\gamma(\omega) = i\cdot\frac{\omega}{c(\omega)}. \tag{11}$$

The strain at section 1 (end of the incident bar) can be computed as

$$\begin{aligned}\tilde{\varepsilon}_1(\omega) &= \tilde{\varepsilon}_1\left(\frac{L_b}{2},\omega\right)\\ &= \tilde{P}_i(\omega)\cdot e^{-\gamma(\omega)(L_b/2)} + \tilde{P}_r(\omega)\cdot e^{\gamma(\omega)(L_b/2)}\end{aligned} \tag{12}$$

and then, written in the time domain using the inverse Fourier transform

$$\varepsilon_1(t) = F^{-1}[\tilde{\varepsilon}_1(\omega)]. \tag{13}$$

In the same way, the strain in section 2 of output bar, located at $x = -L_b/2$, can be stated in the frequency domain as

$$\tilde{\varepsilon}_2(\omega) = \tilde{\varepsilon}_2\left(-\frac{L_b}{2},\omega\right) = \tilde{P}_t(\omega)\cdot e^{\gamma(\omega)(L_b/2)} \tag{14}$$

where $(\tilde{P}_t\omega)$ is the Fourier transform of the measured transmitted pulse. Strain at this section in the time domain is obtained by means of the Fourier inverse transform

$$\varepsilon_2(t) = F^{-1}[\tilde{\varepsilon}_2(\omega)]. \tag{15}$$

Once actual strains at the bar end, $e_1$ and $e_2$, are obtained considering the dispersive nature of the waves, the magnitude of the stress, strain and strain rate can be calculated using Eqs. (6) (8).

The dispersion effect was evaluated by comparing stress strain curves obtained by applying the above-

mentioned corrections and using the conventional theory. Fig. 9 shows both results for a quasi-isotropic laminate tested at room temperature. The tensile strength and failure strain are very close in both curves; the oscillations are different from one to the other but the tendencies are the same. So, it can be concluded that the wave dispersion effect along the bars does no affect significantly the results from a practical view point.

### 3.2. Temperature influence

During a low temperature test, the bars have a temperature gradient with the lowest values at their ends inside the chamber. This gradient would modify elastic wave propagation due to the change of mechanical impedance of the bars, giving rise to multiple reflection that would not occur in a constant mechanical impedance bar.

Experimental techniques to analyse the effect of temperature gradient in bars were developed by Rodríguez [35] and Miguélez [36] with tests at high temperatures on metallic materials. A stress pulse is generated in a single bar with free end, and incident and reflected waves are measured at the central section. The propagation of the elastic wave is studied, with and without temperature gradient, in order to evaluate the effect of impedance variation. In a bar without temperature gradient, the incident and reflected waves should be equal, only their signs varying due to the complete reflection of the wave at the free end, so the addition of both waves should be zero (close to zero regarding dispersive effects). With temperature gradient, incident and reflected pulses will differ because of the impedance variation, and would cause a non-null value in the added waves. According to these authors, if this value is of the same order as that of the noise due to dispersive effects, the impedance variation could be neglected in the signal analysis.

In order to extend this technique to low temperature conditions, similar tests were done at room temperature and at −60 °C. The results showed that the temperature gradient has no noticeable effect on the wave propagation at −60 °C. Fig. 10 shows the addition of incident and reflected waves at both temperatures. The difference between the curves is negligible compared to the magnitude of the incident pulse, and thus no change of bars impedance due to temperature was considered.

### 3.3. Direct strain measurement

Strain in the specimen can be obtained from Eq. (7), as explained above, (neglecting wave dispersion and temperature gradient effects) by means of an indirect technique. The Hopkinson bar set-up has been commonly used with a cylindrical coupon where the wave propagation is close to the one-dimensional case. The composite laminate should also be tested with a flat coupon, which introduces three-dimensional effects that could give rise to wrong values of indirect strain measurement. Therefore, the strain was also measured directly by placing strain gauges (VISHAY CEA-06-1225UN-350) on the specimen, and was compared to that given by Eq. (7).

Fig. 11 shows strain calculated form the elastic waves recorded at the bars, and strain measured directly in the specimen. These results correspond to a quasi-isotropic laminate $[\pm 45/0/90]_S$ tested at room temperature. Both curves are very close during the first 25 ls, the period when the strain gauge is attached to the specimen, and that finishes with the onset of the failure process. Then, fibres begin to break, the gauge debonds, and strain measurement is no longer valid. From both strain measurements, stress strain curves were derived and showed little variation (Fig. 12).

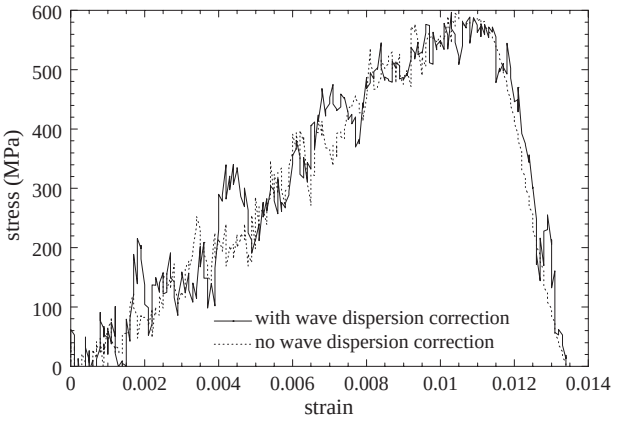


Fig. 9. Stress strain curves of a quasi isotropic laminate [+45/ 45/0/90]$_S$ tested at room temperature with and without wave dispersion correction.

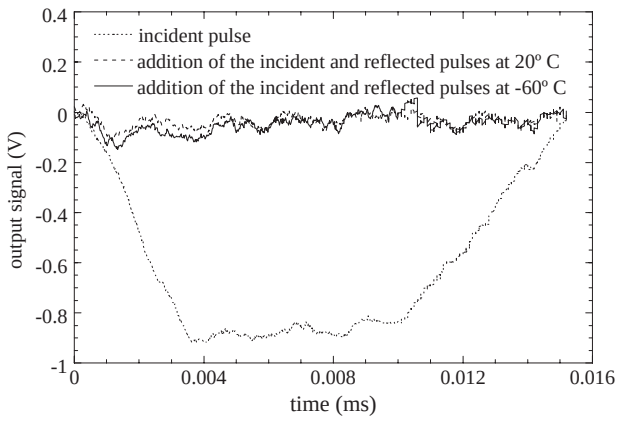


Fig. 10. Incident pulse and addition of incident and reflected pulse for room temperature and 60 °C.

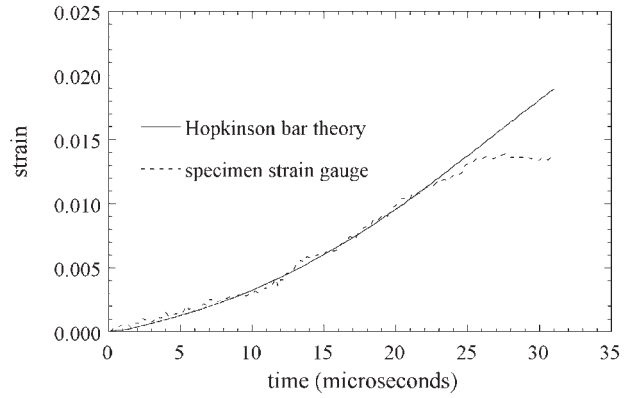


Fig. 11. Strain histories, calculated with the one dimensional theory and measured by means of a strain gauge. Quasi isotropic laminate $[\pm 45/0/90]_S$ at room temperature. Strain rate: 860 $s^{-1}$.

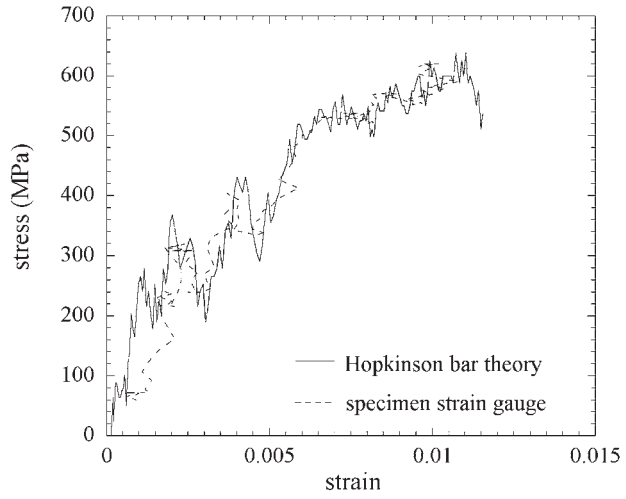


Fig. 12. Stress strain curves calculated with the one dimensional theory and measured by means of a strain gauge. Quasi isotropic laminate $[\pm 45/0/90]_S$ at room temperature. Strain rate: 860 $s^{-1}$.

This analysis was done also at low temperature (using a VISHAY WK-00-250BG-350 strain gage) and similar results for both ways of strain measurements were obtained.

Considering the specific characteristics of the test considered in this work (wave dispersion effects, low temperature, specimen geometry) the convenience is seen of using the conventional Hopkinson bar theory to calculate the stress, strain and strain rates of the specimen by means of Eqs. (6) (8).

## 4. Experimental results

Dynamic tensile tests of CFRP unidirectional laminates, in the fibre direction and transversally, and of quasi-isotropic laminates (loading in 0° direction) were performed at 20 and −60 °C. Three specimens were tested in each case. In order to evaluate the strain rate sensitivity of this materials, the dynamic tensile strength, at around 750 900 $s^{-1}$, was compared to quasi-static ones. These results were obtained by the same work team in a previous study [37].

Figs. 13 15 show dynamic stress strain curves corresponding to materials and temperatures considered. Despite the noise level, characteristic of this kind of tests and similar to that obtained by other authors [23,38] is possible to determine with enough accuracy the peak value, associated to the material strength. When using Split Hopkinson Bar, usually only this property is obtained from the stress strain curves [8,23,38]. Before any stress or strain measurements are credible, equilibrium has to be reached between both bar ends; this needs a few reflections of the waves along the specimen. For the coupon geometry and material used, this condition is not achieved during the elastic response, preventing a proper measurement of stiffness.

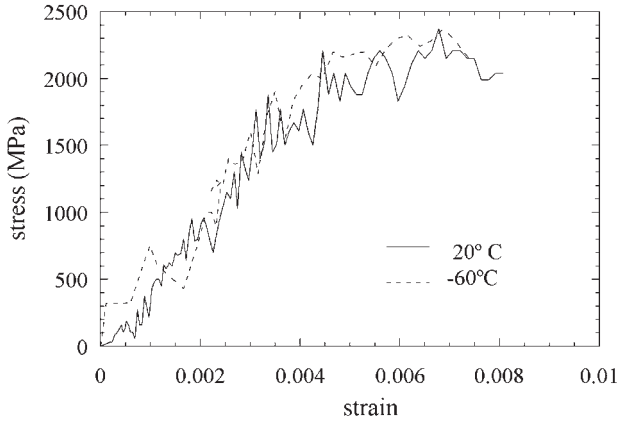


Fig. 13. Stress strain curves for unidirectional laminate $[0]_{10}$ at 20 and 60 °C. Strain rate around 750 $s^{-1}$.

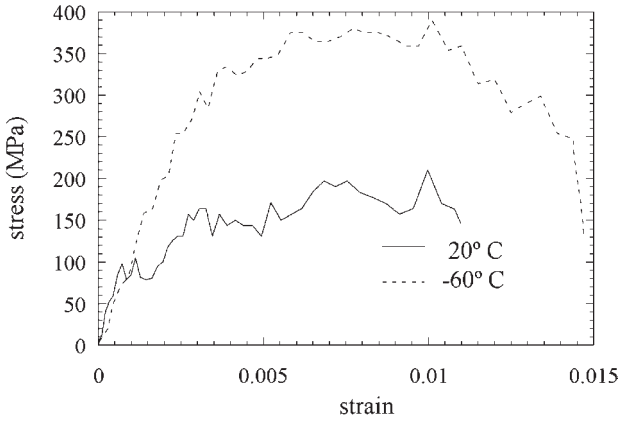


Fig. 14. Stress strain curves for unidirectional laminate $[90]_{10}$ at 20 and 60 °C. Strain rate around 890 $s^{-1}$.

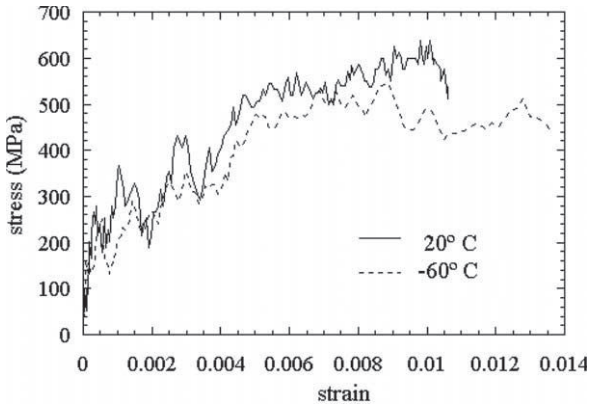


Fig. 15. Stress strain curves for quasi isotropic at 20 and 60 °C. Strain rate around 890 s $^{1}$.

In unidirectional $[0]_{10}$ laminate, the main failure mechanism is fibre breakage both in static and dynamic conditions. Several authors have reported that carbon fibres are no sensitive to strain rate at room temperature [8] and other showed that their static mechanical properties are hardly modified by temperature [39,40]. Thus no variation of the tensile strength is expected for the different testing conditions. Dynamic stress strain curves for $[0]_{10}$ specimens at 20 and −60 °C are presented in Fig. 13. No effect of temperature on the tensile strength was detected. Regarding strain rate influence, dynamic tensile strength is slightly greater than that corresponding to quasi-static conditions (2.14 GPa) [37], although the difference is inside the experimental dispersion.

In contrast, $[90]_{10}$ laminate properties are mainly related to the matrix behaviour. The epoxy resin strength changes at low temperature. Below the principal transition temperature $T_g$ which takes places at around 140 °C, another vitreous transition occurs at low temperature due to the activation and movements of the principal epoxy chains segments. This temperature $T_b$ is close to −40 °C in pure epoxy, falling down to −45 °C when charges are added [41]. $T_b$ is therefore between the two temperatures considered in this study and the laminate should be affected in this load direction. Fig. 14 shows stress strain curves for unidirectional $[90]_{10}$ laminate. In this case the maximum stress increased drastically at low temperature, over 100%. Focusing on strain rate, it affect the properties of this laminate, as has been stated by the experimental results. Dynamic tensile strength is 110% higher than the static value (80 MPa) [37] at room temperature, due to viscous behaviour of the epoxy resin [2,8,41].

The strength of quasi-isotropic laminate is governed by fibre breakage in 0° plies. Thus the effects of temperature and strain rate should be close to that observed in the [0] laminate. As expected, Fig. 15 shows the very slight temperature effect on the dynamic properties for the quasi-isotropic laminate; averaged values of dynamic tensile strengths are the same at both thermal conditions (Fig. 16). Regarding strain rate sensitivity, tensile strength in dynamic conditions (890 s $^{1}$) slightly increases above the corresponding value in quasi-static tests (520 MPa) [37], as Fig. 17 shows. Syed and Brar [38] have found a similar increment, testing at room temperature and 400 s $^{1}$, a AS4/3501-6 $[+45/-45]_S$ laminate. Eskandari and Neme [4], testing a similar laminate at room temperature, found a comparable increment at a strain rate of 145 s $^{1}$.

Regarding the shape of the stress strain curves, the $[0]_{10}$ laminate shows a brittle behaviour with a sudden drop of the stress value. For laminates with fibres oriented in a direction different from zero degrees, the curves show a plateau before failure. This is more noticeable for the $[90]_{10}$ lay-up, in which fibres does not play a role in the strength and the load is carried mainly by the resin, showing ductile behaviour.

The effect of temperature on the tensile properties at high strain rates is summarized in Fig. 16. Laminates with fibres oriented in the load direction are not sensitive to thermal conditions in the range 20 to −60 °C. In contrast, strength greatly increases when failure is matrix driven. Fig. 17 shows the strain rate influence. Tensile strength is slightly affected in laminates whose failure is fibre driven, whereas a great increase is observed in

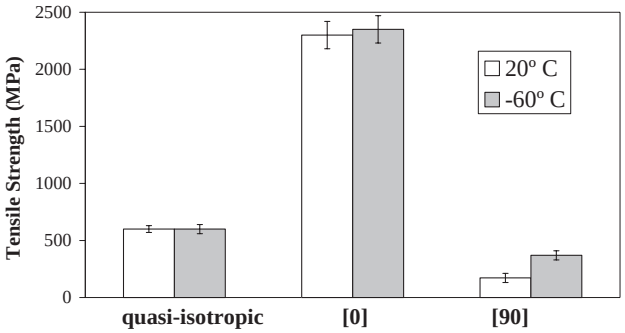


Fig. 16. Dynamic tensile strength at 20 and 60 °C.

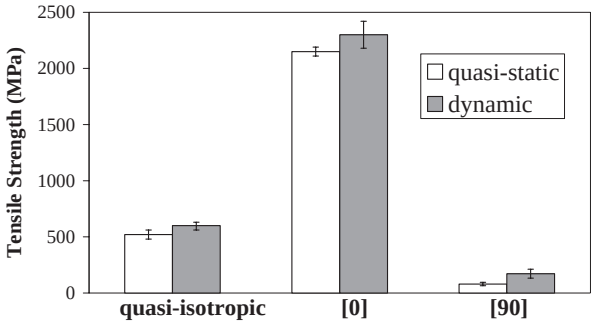


Fig. 17. Strain rate influence at 20 °C in tensile strength.

laminates with 90° oriented fibres due to viscous behaviour of the matrix.

## 5. Conclusions

We studied the dynamic tensile behaviour of CFRPs at low temperature performing split Hopkinson pressure bar test. Both unidirectional and quasi-isotropic laminates were considered.

Among the different specimen fixtures proposed by other authors to test in tension composite laminate with the Split Hopkinson Bar, the gluing technique showed the advantages of avoiding slipping of the laminate, failure at the coupon ends, and noise in the reflected and transmitted waves. This device was used successfully at temperatures down to −60 °C.

The specific characteristic of this kind of tests (impedance variation due to temperature gradient in bars, and three-dimensional effects in bars and specimen) required a detailed analysis of the influence of these effects on stress wave propagation and thus in the hypothesis adopted to determine the stress strain relations. This analysis showed the validity of conventional Hopkinson bar theory, which assumes one-dimensional elastic wave propagation and constant mechanical properties in the bars, to calculate the stress, strain and strain rate.

The results of the dynamic tests showed little influence of temperature and strain rate on the tensile strength of a unidirectional laminate loaded in the fibre direction; in contrast, the strength increases appreciably in the transverse direction at low temperature and high strain rate. Temperature has little effect on the in-plane dynamic properties of the quasi-isotropic laminate considered in this work. Regarding strain rate, a slight increase in tensile strength was observed under dynamic loading. The rheologic behaviour of the epoxy matrix, its phase transformation at low temperature, and the non-sensitivity of carbon fibre to temperature and strain rate explain these experimental results.

## Acknowledgement

The authors are indebted to the Spanish Comisión Interministerial de Ciencia y Tecnología (Project MAT-98/0273) for the financial support of this work.

## References

[1] Tennyson RC. Composites in space challenges and opportuni ties. Proc ICCM 10 1995;1:35 56.
[2] Gilat A, Goldberg RK, Roberts GD. Experimental study of strain rate dependent behaviour of carbon/epoxy composite. Compos Sci Technol 2002;62:1469 76.
[3] Hosur MV, Alexander J, Vaidya UK, Jeelani S. High strain rate compression response of carbon/epoxy laminate composites. Compos Struct 2001;52:405 17.
[4] Eskandari H, Neme JA. Dynamic testing of composite laminates with a tensile split Hopkinson bar. J Compos Mater 2000;34(4):260 73.
[5] Hallet SR, Ruiz C, Harding J. The effect of strain rate on the interlaminar shear strength of a carbon/epoxy cross ply laminate: comparison between experiment and numerical prediction. Com pos Sci Technol 1999;59:749 58.
[6] Hancox NL. Izod impact testing of carbon fibre reinforced plastic. Composites 1971;1:41 5.
[7] Harris B, Beaumont PWR, Moncunill de Ferran E. Strength and fracture toughness of carbon fibre polyester composites. J Mater Sci 1971;6:238 51.
[8] Welsh LM, Harding J. Dynamic tensile response of unidirection ally reinforced carbon epoxy and glass epoxy composites. In: Proceeding of the 5th International Conference on Composite Materials; 1985. p. 1517 31.
[9] Adams DF, Adams LG. A tensile impact test apparatus for composite materials. Exp Mech 1989;29:466 73.
[10] Kolsky H. An investigation of the mechanical properties of materials at very high rates of loading. Proc Phys Soc B 1949;62:676 700.
[11] Li Z, Lambros J. Determination of the dynamic response of brittle composites by the use of the split Hopkinson pressure bar. Compos Sci Technol 1999;59:1097 107.
[12] Tsai J, Sun CT. Constitutive model for high strain rate response of polymeric composites. Compos Sci Technol 2002; 62:1289 97.
[13] Hou JP, Ruiz P. Measurement of the properties of woven CFRP T300/914 at different strain rates. Compos Sci Technol 2000;60:2829 34.
[14] Fu JC, Labbe C, Lataillade JL, Collombet F, Sellier E, Le Petitcorps Y. Propriétés mécaniques des matériaux composites (SiC/2124 et SiC/8090) soumis à des sollicitations en torsion et traction à grande vitesse et à haute température. J Phys IV 1994;Colloque C8:219 24.
[15] Fellows NA, Harding J. Use of high speed photography to study localisation during high strain rate torsion testing of soft iron. Mater Sci Eng A 2001;298(1 2):90 9.
[16] Melin LG, Asp LE. Effect of strain rate on transverse tension properties of a carbon/epoxy composite: studied by Moiré photography. Composites A 1999;30:305 16.
[17] Rubio L. Determinación de parámetros de fractura dinámica a alta velocidad de deformación. PhD Thesis, Department of Mechanical Engineering, Carlos III University; 1999.
[18] Hayes SV, Adams DF. Rate sensitive tensile impact properties of fully and partially loaded unidirectional composites. J Testing Evaluation 1982;10(2):61 8.
[19] Minnar J, Zhou M. Characterization of impact in composite laminates. Shock Compression Condensed Matter 2002:1208 11.
[20] McGee JD, Nemat Nasser S. Dynamic bi axial testing of woven composites. Mater Sci Eng A 2001;317:135 9.
[21] Harding J, Welsh LM. A tensile testing technique for fibre reinforced composites at impact rates of strain. J Mater Sci 1983;18:1810 26.
[22] Harding J, Li YL, Saka K, Taylor EC. Characterization of the impact strength of woven carbon fibre/epoxy laminates. In: International Conference of Mechanics and Properties of Mate rials at High Rates of Strain; 1989. p. 403 10.
[23] Staab GH, Gilat A. Behavior of angle ply glass/epoxy laminates under tensile loading at quasi static and high rates. In: Proceed

ings of the American Society for Composites: Seventh Technical Conference; 1992. p. 1041 50.
[24] Harding J, Ruiz C. The mechanical behaviour of composite materials under impact loading. Key Eng Mater 1998;141 143:403 26.
[25] Schutz JB. Properties of composite materials for cryogenic applications. Cryogenics 1996;38(1):3 12.
[26] Dutta PK. Low temperature compressive strength of glass fibre reinforced polymer composites. J Offshore Mech Artic Eng 1994;116(3):167 72.
[27] Ip KH, Dutta PK, Hui D. Effect of low temperature on the dynamic moduli of thick composite beams with absorbed mois ture.. Composites B 2001;32:599 607.
[28] Adams RD, Singh MM. Low temperature transitions in fibre reinforced polymers. Composites A 2001;32:797 814.
[29] Al Hassani STS, Kaddour AS. Strain rate effects on GRP, KRP and CFRP composite laminates. Key Eng Mater 1998;141 143:427 52.
[30] Rodriguez J, Chocron IS, Martinez MA, Sánchez Gálvez V. High strain rate properties of aramid and polyethylene woven fabric composites. Composites B 1996;27:147 54.
[31] Zukas J. Impact dynamics. New York: Wiley; 1982.
[32] Pochhammer L. Uber die fortpflanzungsgeschwindigkeiten kleiner schwingungen in einem unbergrensten isotropen kreiszylinder. J fur die Reine Angewande Mathematik 1876;81:324 36.
[33] Love AEH. A treatise on the mathematical theory of elastic ity. New York: Dover Publications; 1944.
[34] Bancroft D. The velocity of longitudinal waves in cylindrical bars. Phys Rev 1941;59:588 93.
[35] Rodríguez J. Análisis y desarrollo de metodologías para la obtención de propiedades mecánicas de materiales a altas velocidades de deformación y a alta temperatura. PhD Thesis, Complutense University of Madrid; 1993.
[36] Miguélez, H. Caracterización dinámica de materiales avanzados a latas velocidades de deformación y elevada temperatura. Thesis, Department of Engineering, Carlos III University of Madrid; 1998.
[37] Sánchez Sáez S, Gómez del Río T, Barbero E, Zaera R, Navarro C. Static behaviour of CFRPs at low temperatures. Composites B 2002;33:383 90.
[38] Syed IH, Brar NS. Strain rate sensitivity of graphite/polymer laminate composites. Shock Compression Condensed Matter 2001:693.
[39] Reed RP, Golda M. Cryogenic properties of unidirectional composites. Cryogenics 1994;34(11):909 28.
[40] Carrión JG, Pintado JM, García JL. Obtención de propied ades de comportamiento mecánico en materiales compuestos a temperaturas criogénicas. In: Proceedings of the Spanish National Composite Materials Conference (AEMAC); 1997. p. 321 9.
[41] Delaet M. Influences des vitesses de chargement et de la temperature sur léndommagement et la resistance de composites croises verre/epoxiyde. PhD Thesis, Ecole Nationale Supérieure d'Arts et Métiers, Centre de Bor deaux; 1995.